Molecular-dynamic calculation of the inverse-bremsstrahlung heating of non-weakly-coupled plasmas

N. David, D. J. Spence, and S. M. Hooker
Department of Physics, University of Oxford, Clarendon Laboratory, Parks Road, Oxford OX1 3PU, United Kingdom
(Received 8 July 2004; published 22 November 2004)

A molecular dynamic (MD) code is used to calculate the inverse bremsstrahlung (IB) heating rates of a plasma as a function of density and laser intensity. The code belongs to the class of particle-particle-particle-mesh codes. Since the equations solved by the MD code are fundamental, this approach avoids several assumptions which are inherent to alternative methods, for example those which employ a Coulomb logarithm, and is not restricted to weakly coupled plasmas. The results of the MD code are compared to previously published results for plasmas of low coupling. The results of calculations for dense, moderately coupled plasmas are also presented. An analytic expression for the IB heating rate, based on a fit to the rates calculated by the MD code, is suggested. This expression includes terms nonlinear in the plasma density.

DOI: 10.1103/PhysRevE.70.056411 PACS number(s): 52.50.Jm, 52.65.Yy, 52.38.Dx, 52.27.Gr

I. INTRODUCTION

The question of the rate of energy conversion between a plasma and a laser field is of major importance to nearly every application arising from the interaction of high-intensity laser radiation with matter. A key heating process in such interactions is inverse-bremsstrahlung (IB) heating. As is known from basic electrodynamics [1], every accelerated charge emits electromagnetic radiation, so called bremsstrahlung. The inverse of this effect, absorption of photons by charges undergoing collisions, is called inverse bremsstrahlung. There have been a range of calculations of the IB-heating rate, some of the more important being Schlessinger and Wright [2] in 1979, Polishchuk and Meyer-Ter-Vehn [3] in 1994, and Pert [4] in 1995. Calculations have been performed using the classical as well as the quantum approach, with general agreement within the valid parameter space.

All these calculations incorporate a major assumption. The energy absorption is calculated assuming a collision of two particles of opposite charge in the external electromagnetic field. The momentum transfer resulting from this collision is then integrated over the phase of the electromagnetic wave and over the velocity distribution of the plasma to yield the final heating rate. Since the cross section of a binary Coulomb collision diverges due to the long range effect of the Coulomb force (in the classical as well as in the quantum picture) a cutoff has to be introduced, which results in the so-called Coulomb logarithm, which is generally of the form $\ln\Lambda=\ln(b_{\max}/b_{min})$ [4,5]. The long-range cutoff b_{max} is related to the Debye length of a plasma $\lambda_D=\sqrt{\epsilon_0 T_e/e^2 n_e}$ in which T_e is the electron temperature in J, e the elementary charge, and n_e the electron density in m^{-3}. The short-range cutoff b_{min} is related to the deBroglie wavelength $\lambda_{\text{deBroglie}}=h/\sqrt{3mT_e}$ and the classical distance of closest approach $e^2/(4\pi\epsilon_0 mv^2)$, where m is the electron mass and v the electron speed.

The restriction to two-particle collisions and the concept of an outer cutoff are certainly valid for weakly coupled plasmas. In this regime, the cross section for collisions with three or more particles can be neglected and the number of particles in the Debye sphere is large enough to give statistically meaningful shielding. However, many plasmas of current interest to laser-plasma interactions are not weakly coupled [6–10]. Further, even for moderately coupled plasmas where the number of particles in the Debye sphere,

$$N_{\text{Debye}}=\frac{4\pi}{3}\left(\frac{\epsilon_0 T_e}{e^2}\right)^{3/2}\frac{1}{\sqrt{n_e}}, \tag{1}$$

is of order unity (i.e., <10), these assumptions should be treated with caution. In such cases it is impossible to solve the problem analytically and one has to revert to extensive numerical calculations. We note that the requirement $N_{\text{Debye}}\gg 1$ is equivalent to $\Gamma=e^2/(\epsilon_0\lambda_D T)\ll 1$, where Γ is the plasma coupling parameter. Therefore weakly coupled plasmas are described by a large number N_{Debye} and strongly coupled plasmas are described by a small number N_{Debye}.

In this paper a classical, nonrelativistic molecular dynamic (MD) calculation to investigate IB-heating rates is presented. The molecular dynamic approach has the advantage of being derived from a more fundamental set of equations, with fewer assumptions. One does not need to define a Coulomb logarithm and collisions are inherently treated as many-particle collisions; all that is needed for the nonrelativistic calculation are the electrostatic Maxwell equations and Newton's equations of motion. Consequently, MD calculations can be employed for plasma conditions under which alternative approaches lead to significant errors, as well as providing a reliable test for faster approximations. The major disadvantage of this method is its speed. Since every particle has to be treated individually, and a large number of particles is needed to reach statistically meaningful results, MD codes are slow compared to other approaches. It is therefore of particular importance to use algorithms where the number of steps is a low-order function of the number of particles.

The paper is organized as follows. In Sec. II the particle-particle-particle-mesh (P^3M) method, which underlies our MD code, is described and our implementation of the MD approach is outlined. In Sec. III the results of calculations of the IB heating rate for several plasmas, with a range of cou-

pling constants, are described. Where possible the results are compared with those of earlier calculations. In Sec. IV we discuss the results and suggest an analytic expression for the heating rate found from a fit to the results of the MD calculations. Finally in Sec. V we conclude.

II. MOLECUAR DYNAMIC CALCULATION

P^3M method

Solving the individual force equations for each of the N particles in a system would require $N^2/2$ individual force calculations to be undertaken every integration time step. Since the time resolution has to be very high to ensure that even the hardest collisions are treated correctly, a single time step has to be very short. Overall this would result in a calculation that would last several months for 2×10^4 particles. A large reduction in the number of calculations required can be achieved by employing the particle-particle-particle-mesh (P^3M) method described by Hockney and Eastwood [11]. In this method the force on a particle is divided into a collective, long-range term from the majority of the particles (particle-mesh); and a short range term by the particles close to the particle in question (particle-particle). Using this general idea, we chose to calculate the long range effects by solving the Poisson equation on a mesh, and treating the short-range effects by direct integration of the Coulomb force. The calculations were performed on a 2.4-GHz personal computer and took on average three days for one data point.

A similar approach has recently been used by the authors [12] to calculate the equilibration rate of a non-Maxwellian electron energy distribution. Other recent molecular dynamic calculations have been performed by Batishchev *et al.* [13] and Gibbon [14]. Both of these are based on tree algorithms, using massively parallel computers. Batishchev has used the MD approach for calculating IB heating, but only treats weakly coupled plasmas. The simulations undertaken by Gibbon were focused on transport rather than IB heating.

1. Particle-mesh

In our code the coordinate space is a three-dimensional (3D) cube, represented by a 16^3-point grid. The boundary conditions are chosen to be periodic. The long-range effects are then treated by solving the Poisson equation on the mesh with a fast Fourier transform (FFT) [15]. For each particle the complete charge was assigned to the closest grid point [16].

The system of differential equations to be solved is

$$\Delta\Phi(\vec{x}) = -\frac{\rho(\vec{x})}{\epsilon_0}, \tag{2}$$

$$\vec{E}_p(\vec{x}) = -\vec{\nabla}\Phi, \tag{3}$$

$$m\frac{d\vec{v}}{dt} = q[\vec{E}_p(\vec{x}) + \vec{E}_L], \tag{4}$$

where m is the electron mass, q the electron charge, Φ the electrostatic potential, $\vec{E}_p$ the electric field due to the particles, $\vec{E}_L$ the external laser field, and ρ the charge density. The laser field $\vec{E}_L$ was assumed to be independent of $\vec{x}$ since the length of the simulated cube (i.e., 0.043 μm for $n=10^{20}$ cm^{-3}) is small compared to the laser wavelength (1.06 μm). Note that the size of the cube is still large compared to the Debye length.

Equation (2) is then solved using two FFT's [15]. The calculation time for a FFT is proportional to $N_{\text{cell}} \ln N_{\text{cell}}$, where N_{cell} is the number of cells. Provided that the number of cells is less than the number of particles N, the time to calculate the FFT is very much shorter than that required to solve the $N^2/2$ force equations. A more detailed discussion on the particle-mesh calculation can be found in our earlier work on energy equilibration in plasmas [12].

2. Particle-particle

We chose to use 8000 electrons and 8000 ions for our calculation. With a 16^3-point grid this results in roughly four particles per cell. Each particle responds to a driving electromagnetic wave, and interacts directly with every particle in its own cell or in one of the 26 neighboring cells. This roughly means that every particle interacts directly with its 100 closest neighbors. It interacts with the remaining 15 900 via the grid. At this point one should note that, for the plasmas of interest to this paper, the number of directly integrated interactions far exceeds the number of particles in the Debye sphere, thereby ensuring that there is no artificial cutoff due to the grid. It is very important to allow every particle to interact not only with particles in its own cell, but also with every particle from a neighboring cell: If that was not the case, one could suddenly have one particle crossing the boundary of a cell and appearing right next to another particle that happens to be close to the boundary without ever having felt the close range force between them up to this point. In addition, numerical errors due to calculations on a finite grid are reduced. Since the force scales as $1/r^2$, so do the numerical errors arising from the discreteness of the mesh. By including the neighboring cells in the direct integration, the minimum distance for particle-mesh interaction is now 2 instead of 1, thereby reducing errors by a factor of up to 4.

The integration of the particle-particle interaction is performed by a simple Verlet algorithm [16–20]. Typically an oscillation of the electromagnetic wave was resolved in 2×10^5 time steps, which for 1.06-μm wavelength results in a single time step of $dt\approx1.8\times10^{-20}$ sec. This very short time step is needed to correctly resolve the hardest encounters between particles.

3. Divergence of the Coulomb field and the inner cutoff

Any numerical calculation working with a finite time step is subject to numerical errors. These errors can generally be made sufficiently small by choosing a small enough time step. Yet, this turns out to be slightly problematic for the case of an attractive Coulomb collision, since the field tends to infinity for distances approaching zero. Even for very small time steps there is still a chance that two particles are so close to each other at some point in the calculation that the

time step is then incapable of resolving the motion. This can result in unphysical momentum transfers that violate energy conservation.

To avoid this, a numerical cutoff was introduced, so that the force between two particles could not exceed a certain value. If two particles were within this cutoff the magnitude of the interaction force was set to the value at cutoff distance. The majority of the calculations was performed with an inner cutoff set to $a_0/20$, where a_0 is the Bohr radius. For the plasmas calculated in this paper this is significantly less than the deBroglie wavelength. We emphazise, however, that this is a purely numerical cutoff and it is not to be mistaken with a physical cutoff: the value of the numerical cutoff may be changed, within sensible limits, with essentially no change in the calculated results.

To ensure that our numerical cutoff did not introduce unphysical effects, the program was run several times with different values for the cutoff. It was found that if the cutoff was too large the heating rate decreased, as expected, since a significant number of very hard collisions are artificially reduced in strength. However, smaller cutoffs showed convergence within the expected numercial errors, and hence we conclude that the cutoff successfully stabilizes the numerics without interfering with the physics we are trying to observe.

The physical cutoff that very often appears in this context, namely the inner cutoff of the Coulomb logarithm, is unrelated to this numerical cutoff. We note that the inner cutoff of the Coulomb logarithm b_{min} is related to the deBroglie wavelength of the electron and/or the classical distance of closest approach. The latter is innately incorporated in any MD calculation. The former is not needed in a classical calculation that treats electrons as well as ions as pointlike particles, since the differential scattering cross section $d\sigma/d\Omega$ for the two-particle collision is exactly the same for the unshielded classical two-body collision as for the exact quantum mechanical calculation [20]. Therefore, one could argue that any classical calculation that artificially introduces an inner cutoff related to the deBroglie wavelength should be treated with caution.

III. CALCULATIONS

Most important to every molecular dynamic calculation is the right choice of the initial distribution of particles over velocity and position. This is slightly problematic since there is no analytical solution for this distribution of electrons and ions for moderately coupled plasmas. Even though the plasma density is homogenous on a large scale, it certainly is not on a small scale. The well known effect of Debye shielding for example, leads to local inhomogeneity, as described by the two-particle correlation function. These, and higher order effects, will play a role in moderately coupled plasmas. The only way to create an initial distribution is to start the program with some initial distribution and then run the program in the absence of any applied field to let it equilibrate. Of course one should choose the initial distribution as close to the final one as possible, to ensure a short equilibration time.

For the calculations presented in this paper, this was done the following way. As a start, the ions were put into the box completely randomly. Then the electrons were put in using a random number procedure with the modification that on average an electron was $1/\sqrt{3}$ closer to its nearest ion than it was to its nearest electron. This was done to resemble the shielded distribution. Then a simple velocity scaling algorithm was used to create the velocity distribution. In detail this means that initially both the electrons and the ions were given a Maxwellian distribution of velocities according to the desired temperature. In the next step, the program was run for a certain time, during which there would generally be a relaxation between the kinetic energy and the potential energy, according to whether one or the other was too high or too low relative to the equlibrium distribution. The kinetic energy was then renormalized to the desired temperature, and the program rerun. This was done several times until the kinetic energy was stable within the expected numeric error.

The heating rate was determined by running the calculations for four cycles of the laser field, calculating the increase in the mean energy of the plasma, and hence deducing the rate of increase of electron temperature. Since the rate of IB heating is relatively insensitive to the temperature of the plasma, the small change in temperature ΔT_e is accurately given by $\Delta T_e = R\Delta t$, where R is the heating rate at the initial plasma temperature, and Δt is the interval over which the heating is calculated.

Results

Since the number of particles used is not very large (16 000) statistical fluctuations will still be observable. To get an idea of the magnitude of these fluctuations, two different initial distributions were equilibrated and tested against each other.

In addition, several calculations were done to test the numerics of the code. They included changing the integration time step, changing the numerical inner cutoff and testing for energy conservation in the zero-field case. All these tests were successful. The combined numerical and statistical errors were within a 5% range.

The code was then tested against calculations by earlier authors, namely, Polishchuk and Meyer-ter-Vehn [3] and Pert [4]. These two were chosen because they combine between them a range of earlier approaches and contain comparable data.

The formula derived by Polishchuk and Meyer-ter-Vehn [3] is

$$R = \frac{dT_e}{dt} = \frac{8n_i e^4 Z^2 v_E^2}{3m(4\pi\epsilon_0)^2(v_E^2 + v_e^2)^{3/2}} \ln\Lambda \tag{5}$$

with

$$\ln\Lambda = \frac{1}{4}\ln^2[1+\xi] + \ln\left[\xi + \exp\left(\frac{1}{3}\sqrt{\pi/2}\right)\right] \ln\left[\frac{T_e}{\hbar\omega}\right]$$

and

$$\xi = \frac{m v_E^2}{T_e}.$$

Here ω is the frequency of the laser field, n_i the ion density in m^{-3}, $v_E = |eE|/m\omega$ the electron quiver velocity, E

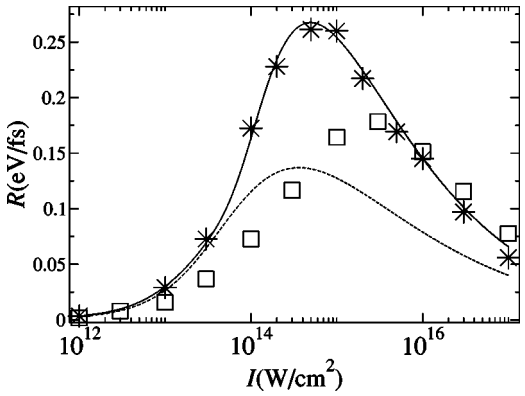

FIG. 1. Comparison of the heating rate R calculated for a plasma with initial values $n_e=10^{20}$ cm^{-3}, $T_e=10$ eV by the formula of Polishchuk and Meyer-ter-Vehn (dashed line) [Eq. (5)], Pert (squares), and the MD code (stars). The solid line shows the heating rate given by the analytic expression suggested in Sec. IV.

$=\sqrt{2c\mu_0 I}$ is the amplitude of the electric field, where I is the intensity of the linearly polarized radiation, $v_e=\sqrt{T_e/m}$ the thermal speed, and Z is the ion charge number. In our case $Z=1$.

The first example plasma is the one chosen by Pert [4]: an electron density of $n_e=10^{20}$ cm^{-3} and an initial temperature of $T_e=10$ eV. The plasma is heated by radiation of wavelength 1.06 μm, corresponding to the Nd:YAG laser transition. For this plasma $N_{\mathrm{Debye}}\approx 5$, a moderately coupled plasma.

Figure 1 compares the rate of increase of electron temperature, R calculated by the MD code with the calculations by Polishchuk and Meyer-ter-Vehn and those by Pert.

It is clear that all three calculations give heating curves of the same form, and are in good quantitative agreement at low intensities. However, the calculated heating rates vary by a factor of up to 2 in the region $\frac{1}{2}mv_E^2 \gtrsim T_e$. For a 10-eV plasma this corresponds to an intensity of $I\approx 4.8\times 10^{13}$ W/cm^2. In detail, the heating rate derived by Pert [4] is in good agreement with our calculation in the limit of high intensity, but the peak heating rate occurs at higher intensities than either that of Polishchuk and Meyer-ter-Vehn [3] or that of the MD calculation. The heating rate calculated by Polishchuk and Meyer-ter-Vehn is lower than the rate calculated by our code for all intensities with $\frac{1}{2}mv_E^2 \gtrsim T_e$.

The difference between the two earlier calculations [3,4] is largely due to a difference in the form of the term resembling the Coulomb logarithm. This also shows one of the weaknesses of those methods; since this term cannot be derived from basic principles there is always a certain amount of arbitrariness associated with it.

One of the key features of all earlier calculations is a linear dependance of the heating rate on the plasma density. However, if three-body collisions (or collisions with even more particles) play a significant role, there should be higher order terms in the density n. To investigate this, the heating of a 10-eV plasma with an electron density of $n_e=10^{19}$ cm^{-3} was calculated. Figure 2 compares the heating rate calculated by the MD code for $n_e=10^{19}$ cm^{-3} with the calculated rates shown in Fig. 1 divided by 10. The rates

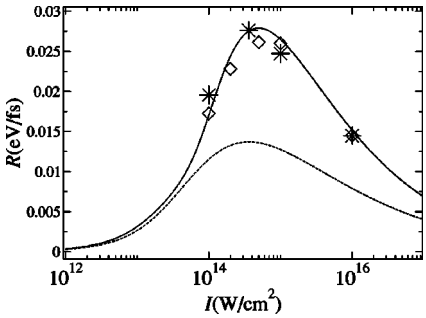

FIG. 2. Comparison of the heating rate R calculated for a plasma with initial values $n_e=10^{19}$ cm^{-3}, $T_e=10$ eV by the formula of Polishchuk and Meyer-ter-Vehn (dashed line) [Eq. (5)], the MD code (stars), dividing the rates calculated in Fig. 1 by 10 (diamonds). The solid line shows the heating rate given by the analytic expression suggested in Sec. IV.

calculated by Polishchuk and Meyer-ter-Vehn and the equation suggested in Sec. IV are also shown.

It can be seen that the scaled rates are close to the directly calculated rates. The heating rates do appear to be just slightly lower than in the $n_e=10^{19}$-cm^{-3} case, but the difference is still inside the error and fluctuation range. This suggests that a density of $n_e=10^{20}$ cm^{-3} is low enough to neglect multiple (>2) particle collisions.

To determine at what density nonlinear effects become significant, the IB heating rate was calculated for two high density plasmas. Figure 3 shows calculated rates for an initial temperature of $T_e=10$ eV and density of $n_e=n_i=5\times 10^{20}$ cm^{-3}. For these conditions $N_{\mathrm{Debye}}\approx 2.5$. Since this coupling is so strong the simulation for Fig. 3 was run with an even shorter time step of $\Delta t\approx 6\times 10^{-21}$ s. Figure 4 shows the calculated heating rates for a plasma with initial temperature $T_e=20$ eV and density $n_i=8\times 10^{20}$ cm^{-3}. In this case $N_{\mathrm{Debye}}\approx 5.5$.

It can be seen that the heating rate decreases relative to the heating rate calculated by Polishchuk and Meyer-ter-Vehn. This becomes especially obvious in the case where $n_i=8\times 10^{20}$ cm^{-3} and the intensity is 10^{14} W/cm^2. Here the MD heating rate is significantly less than the Polishchuk and Meyer-ter-Vehn result. This is a sign of a contribution that is

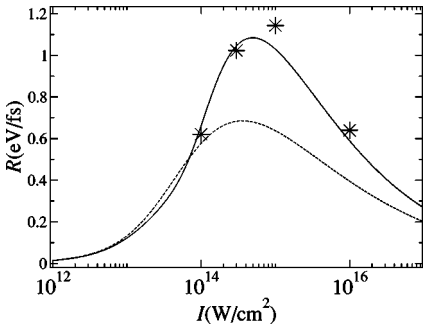

FIG. 3. Comparison of the heating rate R calculated for a plasma with initial values $n_i=5\times 10^{20}$ cm^{-3}, $T_e=10$ eV by the formula of Polishchuk and Meyer-ter-Vehn (dashed line) [Eq. (5)] and the MD code (stars). The solid line shows the heating rate given by the analytic expression suggested in Sec. IV.

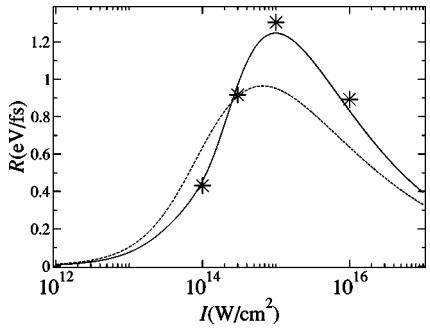

FIG. 4. Comparison of the heating rate R calculated for a plasma with initial values $n_i = 8 \times 10^{20}$ cm^{-3}, $T_e = 20$ eV by the formula of Polishchuk and Meyer-ter-Vehn (dashed line) [Eq. (5)] and the MD code (stars). The solid line shows the heating rate given by the analytic expression suggested in Sec. IV.

nonlinear in the plasma density. This point is discussed in more detail in Sec. IV.

The final plasma for which the heating rate was calculated was one with an initial temperature of $T_e = 5$ eV and a density of $n_i = 10^{19}$ cm^{-3}. This plasma is of interest, since most previous derivations for IB heating rates are not valid for low temperatures. For example, the heating rate calculated by Polishchuk and Meyer-ter-Vehn is only valid for $T_e \gg \hbar\omega$. For the $\lambda = 1.06$-μm radiation considered here, $\hbar\omega = 1.16$ eV, and so this condition is not met.

Figure 5 compares the heating rate calculated for this plasma by the MD code with that calculated by the expression due to Polishchuk and Meyer-ter-Vehn. It is clear that the rate calculated by Polishchuk and Meyer-ter-Vehn underestimates the heating rates in this case. This is largely due the factor in the final term of the Coulomb logarithm, $\ln[T_e/\hbar\omega]$, which obviously breaks down for low temperatures.

IV. DISCUSSION

After comparing earlier results to the MD calculation it appears that two critical things are responsible for the differences: the exact choice of the Coulomb logarithm, and the restriction to two-particle collisions. Since the MD calculation is very slow, and therefore impractical for everyday application, we suggest a modified version of the IB-heating formula from Polishchuk and Meyer-ter-Vehn [3] that fits the MD data.

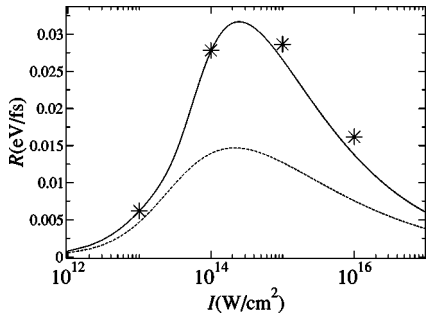

FIG. 5. Comparison of the heating rate R calculated for a plasma with initial values $n_e = 10^{19}$ cm^{-3}, $T_e = 5$ eV by the formula of Polishchuk and Meyer-ter-Vehn (dashed line) [Eq. (5)] and the MD code (stars). The solid line shows the heating rate given by the analytic expression suggested in Sec. IV.

We chose to fit an analytical expression that resembles the result of Polishchuk and Meyer-ter-Vehn:

$$R = \frac{dT_e}{dt} = \frac{8e^4 Z^2 v_E^2}{3m(4\pi\epsilon_0)^2 (v_E^2 + v_e^2)^{3/2}} \alpha(n_i) \ln\Lambda \tag{6}$$

with

$$\alpha(n_i) = C_1 n_i \left(1 - \frac{n_i}{C_2}\right) \tag{7}$$

and

$$\ln\Lambda = \ln\left[C_3\xi + C_4\xi^2 + C_5\xi^3 + \exp\left(\frac{1}{3}\sqrt{\pi/2}\right)\right] \times \ln\left[\exp(1) + \frac{T_e}{\hbar\omega}\right],$$

where

$$\xi = \frac{m v_E^2}{T_e}.$$

The rationale for the modifications to the expression derived by Polishchuk and Meyer-ter-Vehn is as follows. In the expression for the Coulomb logarithm the term $\ln[T_e/\hbar\omega]$ was modified to $\ln[\exp(1) + T_e/\hbar\omega]$ to stablilize this term when $T_e \simeq \hbar\omega$. In the limit of low electron temperatures this term now tends to unity. The remaining terms in ξ were then replaced by a power series in ξ up to ξ^3. The term $\exp(\frac{1}{3}\sqrt{\pi/2})$ was kept to ensure convergence of the two formulas in the low field limit where the results of the MD calculations are in good agreement with the formula due to Polishchuk and Meyer-ter-Vehn. The effect of multiple particle collisions was accounted for by replacing the linear dependance on density by a term of the form $\alpha(n_i) = C_1 n_i (1 - n_i/C_2)$.

The constants C_1, C_2, C_3, C_4, C_5 were then determined by numerically fitting the best curve to all the heating rates calculated by the MD code presented in Figs. 1–5.

It was found that the best fit was achieved for

$$C_1 = 1.089,$$

$$C_2 = 2.211 \times 10^{27} \text{ m}^{-3},$$

$$C_3 = 1.042,$$

$$C_4 = -0.233,$$

$$C_5 = 0.139.$$

It should be noted that the constants C_1 and C_3 are both close to unity such that our suggested formula agrees closely with that of Polishchuk and Meyer-ter-Vehn in the limits of low intensity and low density.

In order to demonstrate the non-linear dependance of the heating rate on the plasma density, Fig. 6 shows the MD

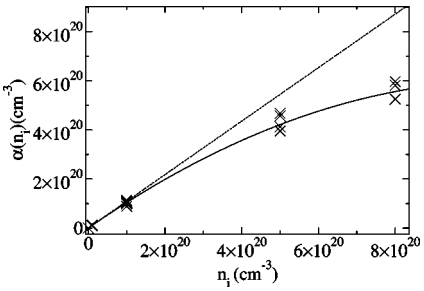

FIG. 6. Values of $\alpha(n_i)$ deduced by dividing the MD heating rate by the rate calculated by Eq. (6), but with $\alpha(n_i)$ set to unity (crosses). These values may be compared with Eq. (7) calculated with $C_2 \rightarrow \infty$ (dashed line) and the fitted value of $C_2 = 2.211 \times 10^{27}$ m^{-3} (solid line).

heating rate divided by the right hand side of Eq. (6), but with $\alpha(n_i)$ set to unity. This procedure yields deduced values for $\alpha(n_i)$ which can be compared to Eq. (7) with and without the nonlinear term. It is clear that $\alpha(n_i)$, and hence the heating rate, increases sublinearly with the plasma density. The deduced value of $C_2 = 2.211 \times 10^{21}$ cm^{-3} shows that the heating will vary nonlinearly with plasma density for plasmas with densities greater than $\approx 5 \times 10^{20}$ cm^{-3}. The nonlinear dependance of the heating rate on plasma density is likely to be caused by the increasing importance of three- (and more) body collisions at high density.

V. CONCLUSION

In summary, we have described a molecular dynamic code for calculating the rate of inverse bremsstrahlung heating of a plasma.

The results of calculations of the IB heating rate as a function of laser intensity were presented for a range of plasma conditions. It was shown that the MD code is in qualitative agreement with ealier work, but differing in details by factors of up to 2 depending on the plasma conditions.

The results of the MD code suggest that the heating rate increases lower than linearly for plasma densities greater than approximately 5×10^{20} cm^{-3}.

Finally an analytic expression was fitted to the results of the MD calculations to yield a formula for the heating rate that could be incorporated into larger plasma codes.

ACKNOWLEDGMENTS

The authors would like to acknowledge helpful discussions of this problem with Professor S. J. Rose and Professor J. S. Wark. S.M.H. is grateful to the Royal Society for financial support, and N.D. to the Rhodes Trust for financial support.

[1] J.D. Jackson, *Classical Electrodynamics* (Wiley, New York, 1998).
[2] L. Schlessinger and J. Wright, Phys. Rev. A **20**, 1934 (1979).
[3] A. Y. Polishchuk and J. Meyer-Ter-Vehn, Phys. Rev. E **49**, 663 (1994).
[4] G. J. Pert *et al.*, Phys. Rev. E **51**, 4778 (1995).
[5] D. O. Gericke *et al.*, Phys. Rev. E **65**, 036418 (2002).
[6] D. J. Spence *et al.*, J. Opt. Soc. Am. B **20**, 138 (2003).
[7] A. Butler *et al.*, Phys. Rev. Lett. **89**, 185003 (2002).
[8] D. J. Spence *et al.*, J. Phys. B **34**, 4103 (2001).
[9] G. J. Pert, J. Phys. B **32**, 27 (1999).
[10] G. J. Pert, J. Phys. B **34**, 881 (2001).
[11] R. Hockney and J. Eastwood, *Computersimulations using Particles* (McGraw-Hill, New York, 1981).
[12] N. David and S. M. Hooker, Phys. Rev. E **68**, 056401 (2003).
[13] O.V. Batishchev *et al.*, 30th EPS Conference on Controlled Fusion and Plasma Physics, St. Petersburg ECA 2003, Vol. 27A, Sec. 3.72 (unpublished).
[14] P. Gibbon *et al.*, Phys. Plasmas **11**, 4032 (2004).
[15] W. H. Press *et al.*, *Numerical Recipes in C* (Cambridge University Press, Cambridge, England, 1992).
[16] C. K. Birdsall and A. B. Langdon, *Plasma Physics via Computer Simulation* (IOP, New York, 1995).
[17] H. J. Kull, *Computersimulation von Plasmen, Skriptum zur Vorlesung* (RWTH Aachen, Aachen, 2001).
[18] F. John, *Partial Differential Equations* (Springer, New York, 1978).
[19] W. Ames, *Numerical Methods for Partial Differential Equations* (Academic, New York, 1992).
[20] E. Merzbacher, *Quantum Mechanics* (Wiley, New York, 1998).